







Research Article

Do ice-dam rupture events leave a distinctive signature in proglacial lake sediments?

Guido Brignone^a , Matias Romero^{a,b,c} , Maximillian Van Wyk de Vries^{d,e,f} , Emi Ito^{d,g} , Mark Shapley^g  and Eduardo Luis Piovano^{a,b} 

^aFacultad de Ciencias Exactas, Físicas y Naturales (FCEfYN), Universidad Nacional de Córdoba, Córdoba, X5016GCA, Argentina; ^bCentro de Investigaciones en Ciencias de la Tierra (CICTERRA), Consejo Nacional de Investigaciones Científicas y Tecnológicas (CONICET), Córdoba, X5016GCA, Argentina; ^cDepartment of Geoscience, University of Wisconsin-Madison, Madison, Wisconsin 53706, USA; ^dDepartment of Earth and Environmental Sciences, University of Minnesota, Minneapolis, Minnesota 55455, USA; ^eSaint Anthony Falls Laboratory, University of Minnesota, Minneapolis, Minnesota 55455, USA; ^fSchool of Geography and the Environment, University of Oxford, Oxford OX1 3QY, UK and ^gContinental Scientific Drilling Facility, Department of Earth and Environmental Sciences, University of Minnesota, Minneapolis, Minnesota 55455, USA.

Abstract

Lake sediment provides a valuable record of past environmental change. However, the controls on sedimentation in proglacial lakes and their relation to glacier retreat remain poorly understood. In this study we analyze glaciolacustrine sediment production and deposition in Canal de los Témpanos, Lago Argentino, Argentine Patagonia. We associate temporal changes in the sedimentologic and geochemical characteristics analyzed from Lago Argentino cores with Late Holocene fluctuations of the Perito Moreno and Ameghino glaciers. We show that the dominant sediment source at our study site switched from Ameghino to Perito Moreno Glacier after the recession of Ameghino Glacier and the formation of the marginal ice-contact lake into which it currently calves. Spectacular ice-dam rupture events generated by Perito Moreno Glacier redistribute large volumes of water through the lake system but do not leave a significant sedimentary signature. Our results demonstrate that a detailed analysis of sedimentologic, petrophysical, and geochemical changes in lake cores can provide insight into regional glacial dynamics and sedimentary processes even in complex systems with multiple competing glacial sources and that changing glacier geometries during retreat can provide insights into the provenience of the sediments.

Keywords: Proglacial lakes, glaciers, Canal de los Témpanos, laminated sediments, sandy bands, Little Ice Age, ice-dam, outburst events

INTRODUCTION

Lakes are one of the most dynamic natural systems, with sediment composed of clastic, chemical, and biological fractions, making them one of the richest paleoenvironmental archives. By trapping sediment, they record past environmental and climatic changes that have taken place within the waterbody and in its basin during its existence (Smol, 1992; Cohen, 2003). Proglacial lakes, which may be in direct contact with glaciers or linked by a proglacial drainage system, are dominated by clastic glacial sediment (Carrivick and Tweed, 2013; Carrivick et al., 2020). The area and volume of proglacial lakes has increased by about 50% globally during the last three decades (Shugar et al., 2020; Sutherland et al., 2020). These lakes strongly depend on the regional climate, the type and scale of glaciers in their basin, and their local geology and dam type (Tweed and Carrivick, 2015). Proglacial lake sedimentation is controlled on a first order by the proximity of the glacier front and fluvial input. The bulk density of turbid sediment inflows determines its position and dispersal within the water column. The final sediment distribution is further affected

by sediment grain size and settling velocity, as well as lake mixing processes (Van Wyk de Vries et al., 2021, 2022).

Although there are multiple studies of proglacial lakes in the literature, their relation to glacier retreat and sediment dynamics is not yet completely understood. Even though glacial lake outburst floods are increasingly frequent due to accelerated glacier melting during the last few decades and they pose a risk to local communities and associated infrastructure downstream (Harrison et al., 2018; Veh et al., 2020), few studies have focused on the sedimentary signature created by past catastrophic events (Piret et al., 2022). In this study we show that sediments deposited in proglacial lakes represent a rich and complex climatic archive and that they can record both short- and long-term patterns of glacier change, but that their registration of extreme hydrologic events may defy expectations.

We investigated post-Little Ice Age (LIA) glacial and sedimentary changes from a lacustrine perspective by studying two gravity and two piston cores from Canal de los Témpanos, one of the main conveyors of water and sediment from the Southern Patagonian Ice Field (SPI) to Lago Argentino in southern Argentina (Fig. 1). Owing to its proximity to glaciers, the sediment record allows insight into the evolution of the glaciers in the region and contributes to a broader understanding of their dynamics.

We carried out a detailed sedimentologic description, granulometric analysis, and compositional analyses (X-ray fluorescence,

Corresponding author: Guido Brignone; Email: guidobrignone96@gmail.com
Cite this article: Brignone G, Romero M, Van Wyk de Vries M, Ito E, Shapley M, Piovano EL (2025). Do ice-dam rupture events leave a distinctive signature in proglacial lake sediments? *Quaternary Research* 123, 70–82. <https://doi.org/10.1017/qua.2024.39>



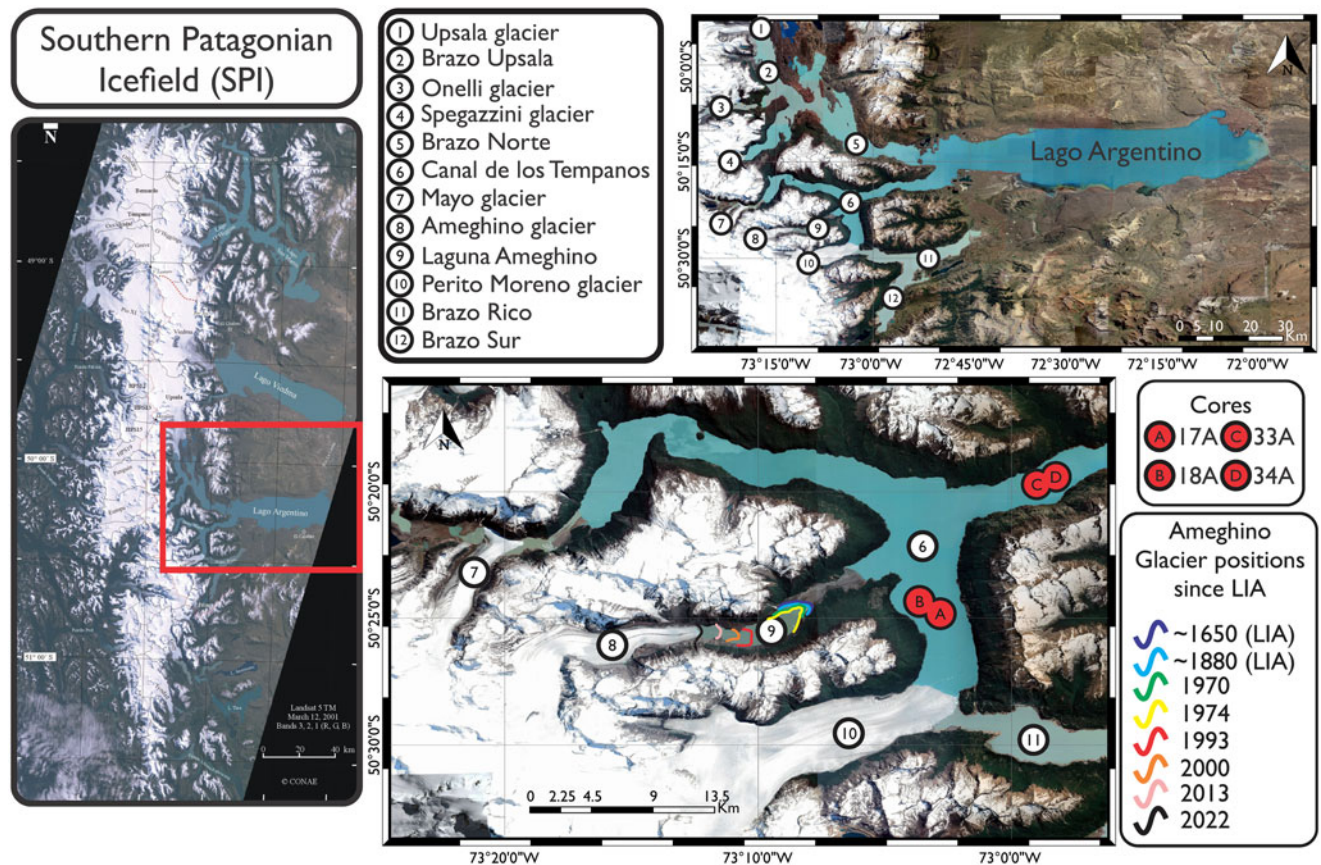


Figure 1. Location of the study area within the Southern Patagonian Ice Field and position of the glaciers in Lago Argentino basin and the sedimentary cores in Canal de los Témpanos. Post-Little Ice Age (LIA) retreat of Ameghino Glacier is also shown.

XRF) of these core sediments. With these data, we evaluate the relative importance of sediment contributions from large lake-terminating glaciers in southwestern Lago Argentino and test our initial working hypothesis: The energetic Perito Moreno ice-dam outburst events would provide a dominant sedimentary signature in proximal Canal de los Témpanos locations.

Since the beginning of the twentieth century, repeated ice-damming events (23 outburst events since the first occurrence until the coring campaign; Supplementary material no. 4) have produced recurring large floods by impounding the southernmost branches of the lake and then, during ice-dam failure, releasing great surges of water towards Canal de los Témpanos producing a sudden lake-level rise (Pasquini & Depetris, 2011; Richter et al., 2016).

Previous studies have elucidated (1) seasonal fluctuations in glacial melt, temperature, and fluvial discharge contributing in varying degrees to the formation of varves across the lake basin (Van Wyk de Vries et al., 2021, 2022); (2) temporal changes in the sediment mass accumulation rate and sediment pixel intensity recording paleoclimate in the Lago Argentino region, including resolving the local periodicity of the Southern Annular Mode (Van Wyk de Vries et al., 2023a); and (3) proposed climatic controls on sedimentation across different zones of Lago Argentino (Van Wyk de Vries et al., 2023b). Here we aim to provide a detailed case study of the effect of changes in glacier extent on sedimentation in a multisource lake system, and understand what the advantages and challenges are of using this understanding for paleoenvironmental reconstruction.

BACKGROUND AND REGIONAL SETTING

Lago Argentino is the largest ice-contact lake located in the SPI, Argentina, which hosts multiple lake-terminating glaciers (Fig. 1; Van Wyk de Vries et al., 2022). The majority of these glaciers have recently thinned and receded in response to climate warming since the LIA (Davies and Glasser, 2012). Historical records and remotely sensed data have allowed monitoring the magnitude of such changes throughout the twentieth and twenty-first centuries, and reveal both high and accelerating ice loss in the Lago Argentino basin (Abdel Jaber et al., 2019; Van Wyk de Vries et al., 2023c). Geologic data retrieved from moraines (Strelin et al., 2014; Kaplan et al., 2016) and tree rings (Mercer, 1968; Aniya, 1996; Masiokas et al., 2009) in the Lago Argentino region provide a broader and longer term context of glacial and climatic fluctuations in the pre-observational era.

Lago Argentino is a hydrologically open, ultra-oligotrophic proglacial lake located in the Andean region of the province of Santa Cruz, Argentina (49.9–50.7°S/72–73.3°W), at 185 meters above sea level (Richter et al., 2016; Goyenechea, 2017). Its maximum depth is greater than 600 m (Sugiyama et al., 2016; Magnani et al., 2019). The current morphology of Lago Argentino is the result of the glaciations that occurred since the Miocene/Pliocene transition (Rabassa et al., 2005). The local climate is characterized by strong westerly winds (southern westerly winds), with greatest wind speeds during the summer (Garreaud et al., 2009). Rainfall is heavy on the western flank of the Patagonian Andes, with annually averaged values of around

5 m, but decreases markedly towards the east to about 200 mm per year in El Calafate (Garreaud et al., 2013; Lenaerts et al., 2014).

Sedimentation for most parts of Lago Argentino is varved (annually laminated), mainly controlled by seasonal changes in glacially sourced sediment and fluvial input, as well as seasonal changes in lake mixing (Van Wyk de Vries et al., 2021, 2022). The eastern part of the lake is a 60-km-long basin elongated in a west–east direction and more than 16 km wide (Strelin and Malagnino, 1996). Towards the west, the basin presents multiple *brazos*, valleys that are structurally controlled and deepened by glacier erosion that make up the eastern terminations of the SPI. The Upsala, Perito Moreno, and Spegazzini glaciers calve directly into Lago Argentino, while the Onelli, Ameghino, and Mayo glaciers each calve into their own proglacial lake (Fig. 1). These proglacial lakes are separated from Lago Argentino either by glaciofluvial plains or by dams created by previously deposited moraines. Rio La Leona drains Lago Viedma into the eastern part of Lago Argentino, while Rio Santa Cruz drains Lago Argentino into the Atlantic Ocean.

Perito Moreno Glacier (50°29'S; 73°04'W; Fig. 1, #10) is one of the largest outlet glaciers of the SPI, with a surface area of 259 km², reaching Lago Argentino at the intersection between Canal de los Témpanos and Brazo Rico (Fig. 1, #6 and #11). Its current extent indicates that it advanced past its LIA position but did not record major advances/recessions during the last 4000 years (Aniya and Skvarca, 1992, 2012; Rott et al., 2004; Masiokas et al., 2009; Sugiyama et al., 2011; De Angelis, 2014). Aniya and Skvarca (2012) collected samples for ¹⁴C dating from the shore of Brazo Sur and Brazo Rico (Fig. 1, #11 and #12), and they concluded that Perito Moreno advanced in 1650 CE, while generating an ice-dam that submerged trees that had been developing on the lakeshore for at least a few hundred years. These authors also determined that during the LIA, Perito Moreno Glacier advanced twice, first, in 1650 CE and again, between 1820 CE and 1850 CE.

Ameghino Glacier (50.45°S, 73.3°W; Fig 1, #8) is located 9 km west of Canal de los Témpanos, and its front calves directly into an ice-contact lake called Laguna Ameghino (Fig. 1, #9). This lake is connected to Canal de los Témpanos by a 3-km-long proglacial river and an outwash plain (Warren, 1994; Aniya and Sato, 1995). According to Aniya (1996), frontal moraines located in this outwash plain are thought to be records of Neoglacial advances. The eastern margin of Laguna Ameghino is defined by the LIA moraines (1600–1700 CE) (Warren, 1994; Aniya and Sato, 1995; Aniya, 1996), based on ¹⁴C dates obtained from trees on trimlines nearby. At that time, the Laguna Ameghino did not exist since its basin was occupied by ice, and the sedimentary material mobilized by the glacier was transported as fluvio-glacial sediments onto the outwash and, through it, to Canal de los Témpanos. This glacier thinned following construction of the LIA moraines and, between 1870 CE and 1880 CE (Warren, 1994; Aniya 1996), allowed the progressive development of Laguna Ameghino, which increased its size due to accelerated glacier shrinkage after 1967 CE (Fig. 1; Minowa et al., 2015).

METHODS

Core acquisition

We used the 108 m of core recovered from 47 sites during the austral winter of 2019 using a combination of a Kullenberg coring

system and a gravity coring system deployed onboard a local ferry. Core recovery ranged up to ~6.5 m, with coring locations distributed across the main lake basin and brazos (glacial fjords). The coring sites were chosen according to a reflection seismic survey (Magnani et al., 2019; Fedotova and Magnani, 2021) that preceded the coring operation. In this study, we selected a subset of four cores recovered from the southwesterly branch of Lago Argentino, Canal de los Témpanos. We selected cores from locations that we thought were most likely to contain records addressing the influence of known outburst flooding on sedimentation patterns.

Core processing

At the Continental Scientific Drilling Facility (CSD Facility), we carried out whole-core scans of magnetic susceptibility, gamma-beam density, and P-wave velocity, then split the cores and imaged them, employing a 20 pixels/mm resolution Geotek Geoscan-III optical line-scanner. Moreover, we performed near-ultraviolet to near-infrared spectrophotometric and magnetic susceptibility scans on the split core surface with a Geotek MSCL-XYZ scanner. We described sediment properties, lithologic units, and sediment structures using the logging software PSICAT (Reed, 2007) following the criteria established by Schnurrenberger et al. (2003). During visual lithologic description, smear slides were made and examined under a petrographic microscope using plane- and cross-polarized light. Smear slides were made from visually distinct portions of the cores to examine minerals, grain characteristics, and any other material contained in the sediment.

Grain-size analysis

We performed 194 laser-diffraction particle size analyses (LD-PSA) of 66 selected core intervals using a Horiba LA-920 LD-PSA. Each sample was measured two to three times in order to test reproducibility. In addition, we measured the standard Aluminum Oxide # 240 at the beginning and at the end of each working day to check for instrument drift over time. No sample pre-processing was needed due to the extremely low concentration of biogenic material. We selected sampling locations that visually appeared representative of different sediment packages, trying to capture all grain sizes present in the cores.

X-ray fluorescence

A COX Analytical Systems ITRAX XRF Core Scanner with a Cr source at the Large Lakes Observatory, University of Minnesota, Duluth, was used to obtain elemental composition and X-radiographic images on split cores. For XRF, a 1-cm-wide central swath of the split core section was scanned, and measurements were taken every 10 mm for cores 33A and 34A. Cores 17A and 18A were scanned at a 5 mm resolution. We focused on elements Si, K, Ca, Ti, Mn, and Fe. Calcium was chosen as the most likely indicator of plagioclase; Si, K, Ti, and Fe were chosen as source indicators, while Mn was used as a redox indicator. The X-radiographic images were taken at a 200 µm resolution (5 pixels/mm) after the XRF scan on the same 1-cm-wide swath. Each elemental signal intensity was normalized by dividing by total counts per second.

Table 1. General information about the cores

Core name (abbreviation)	Coring technique	Location	Sections	Length (m)	Water depth (m)
GCO-LARG19-17A-1K (17A)	Piston	50°24'45"S; 73°2'52"W	1	1.255	173
GCO-LARG19-18A-1 G (18A)	Gravity	50°24'35"S; 73°3'5"W	1	0.65	173
GCO-LARG19-33A-1K (33A)	Piston	50°19'37"S; 72°58'49"W	3	4.3	530
GCO-LARG19-34A-1 G (34A)	Gravity	50°19'30"S; 72°58'35"W	1	0.76	530

RESULTS

Cores

Here we present the general characteristics of the sedimentary cores retrieved from Canal de los Témpanos (Table 1), and results obtained from sediment description (Figs. 2 and 3), magnetic susceptibility (Fig. 4) and density measurements, grain-size analysis (Figs. 5 and 6, Supplementary material no. 1), and XRF analysis (Fig. 7, Supplementary material no. 2).

The cores consist of two pairs, cores 17A and 18A, and cores 33A and 34A. The cores 17A, 18A, and 34A each have one section, while 33A has three, labeled 33A-1 (1.41 m), 33A-2 (1.33 m), and 33A-3 (1.37 m) from the top to the bottom.

Initial core description

Cores 33A and 34A (Fig. 2) consist of layered detrital sediments, from submillimeter-thick laminae to bands over 5 cm thick. Sediments show a near-absence of carbonate minerals, biogenic silica, and organic matter. Magnetic susceptibility presents a variable pattern along these cores, fluctuating from $11.6 \text{ SI} \times 10^{-5}$ to $578.7 \text{ SI} \times 10^{-5}$, while gamma density shows a similar pattern, with values ranging from 1.69 to 2.29 g/cm^3 .

The sedimentary record in 33A shows the presence of coring artifacts or deformations that affect and modify the original properties of the sediments. The most evident example is found within the upper 67 cm of section 33A-2 where the sediment was subject to vertical faulting that resulted in a ~ 2 to ~ 3 cm offset of the left side relative to the right, as viewed in core images (Fig. 2).

Similarly to cores 33A and 34A, the sediments in 17A and 18A (Fig. 3) are detrital and devoid of carbonates and organic matter. Magnetic susceptibility values are between 9.1 and $122.2 \text{ SI} \times 10^{-5}$, while gamma ray density ranges between 1.91 and 2.32 g/cm^3 . The sediments of 17A comprise massive silt with occasional sandy bands and laminated intervals of silt. Towards the base of the core there are intervals of clayey silt laminae (from 99 to 121 cm). Sedimentary structures display coring artifacts along the entire length of the core. The upper interval of the core was lost due to difficulties during coring, and the length of the missing material is unknown. Core 18A is composed of clayey silt laminae with sandy silt laminae and silt bands towards the bottom. Visible deformations or coring artifacts occur between 48 cm and the bottom of the core at 60 cm, where the layers are tilted and thickened relative to undeformed intervals.

Laminated sediments

These units are dominated by bundles of clayey silt laminae intercalated with sandy silt layers. The sandy silt layers are normally graded, ranging from <1 to 10 mm thick, with sharp basal and diffuse upper contacts.

The magnetic susceptibility measurements recorded a maximum value of $136.4 \text{ SI} \times 10^{-5}$, a minimum of $11.6 \text{ SI} \times 10^{-5}$, and an average of $35.99 \text{ SI} \times 10^{-5}$.

We identified three subunits based on abundance of sandy silt layers along the longest core, 33A (Fig. 2): (a) laminated clayey silt alternating with normally graded sandy silt layers; (b) laminated clayey silt with sandy silt bands; and (c) laminated clayey silt.

Sandy bands

These units consist of normally graded sandy bands and laminations ranging from 5 mm to >5 cm thick. They exhibit sharp and diffuse contacts at the bottom and top, respectively (Figs. 2 and 3).

Sandy bands are present in cores 33A, 34A, and 17A. In sections 33A-2 and 33A-3, there are sets of successive bands, while in the upper section 33A-1, single band units are observed. Additionally, the abundance of sandy bands decreases towards the top of the core. The thickness, grain size, and magnetic susceptibility values of these sandy bands also decrease upsection (Fig. 4).

These sandy bands have the highest magnetic susceptibility values of the cores, ranging from $25.6 \text{ SI} \times 10^{-5}$ to $578.7 \text{ SI} \times 10^{-5}$, with an average of $174.35 \text{ SI} \times 10^{-5}$.

Grain-size analysis

In cores 33A and 34A, grain-size values range from clay ($<3.9 \mu\text{m}$) to medium sand ($>250 \mu\text{m}$) (Figs. 2 and 5). The laminated unit is mostly dominated by clayey silt, but with a variable abundance of sandy silt layers intercalated within the finer sediments. The coarsest sediments in these cores are represented by the sandy bands whose grains can reach over $400 \mu\text{m}$ in diameter.

The other cores, 17A and 18A, contain sediments ranging from clay ($<3.9 \mu\text{m}$) to medium sand ($>250 \mu\text{m}$) (Figs. 3 and 6). They present laminated clayey silt sediments with sporadic submillimetric-thick sand laminae, coarser massive silt, and sandy bands.

X-ray fluorescence

For 33A and 34A, calcium (Ca) values decrease from the deepest sediments in section 33A-3 to the shallowest in core 34A, with maximum values in the sandy bands. Potassium (K), on the other hand, shows opposite fluctuations, with increasing values from the oldest to the most modern sediments, with minimum values in the sandy bands. Titanium (Ti) and silicon (Si) values show a similar behavior, with no clear trend along the sedimentary record, although a small decrease in Ti and a slight increase in Si are observed towards section 33A-1 and core 34A. In some sandy bands of section 33A-3, the values of both elements are minimal (especially for Si), while in the sandy bands in 33A-1

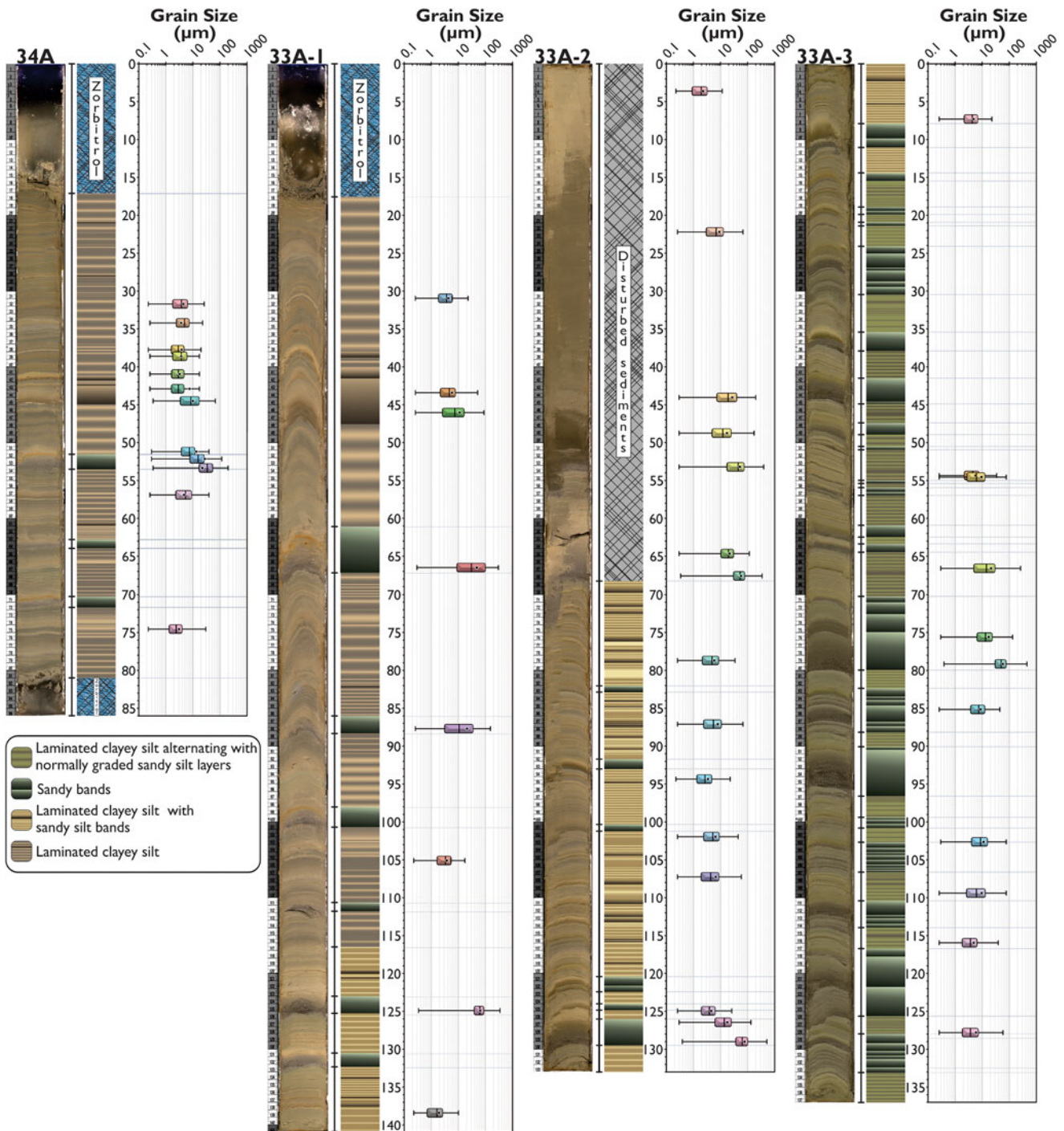


Figure 2. Core 34A (left) and 33A (right). From left to right: the core image, sediment units, stratigraphic column, and profile of grain-size boxplots. Presented is the analysis carried out on the different units (delineated by dashed lines on the profiles) present in these cores, from silt-to-sand bands to clayey silt laminae. A decrease in grain size is observed from the deepest section (33A-1) to the upper sediments (33A-1 and 34A). Note that the sand fraction can be underrepresented due to the technique used.

and 34A they are maximal. The Mn/Ti and Fe/Ti ratios show close patterns and do not vary significantly between the laminated sediments and sandy bands in 33A-3 and 33A-2. However, in younger sediments in 33A-1 and 34A, the sandy bands exhibit the lowest Mn/Ti and Fe/Ti values, with the trend more noticeable for the Fe/Ti ratios.

In cores 17A and 18A, no marked tendencies were found for the elements analyzed along the sedimentary record, but lower

values of Ca and Ti together with increases in K and Si were identified in some sandy bands of core 17A. In core 18A, the massive silt shows maximum values of Ca and minimum values of Si and Ti. The Mn/Ti and Fe/Ti values show similar variations, with greater fluctuations of Mn/Ti in 18A, while the highest values for both ratios are associated with the sandy bands in core 17A and the massive silt in 18A. We present our full XRF results in Supplementary material no. 3.

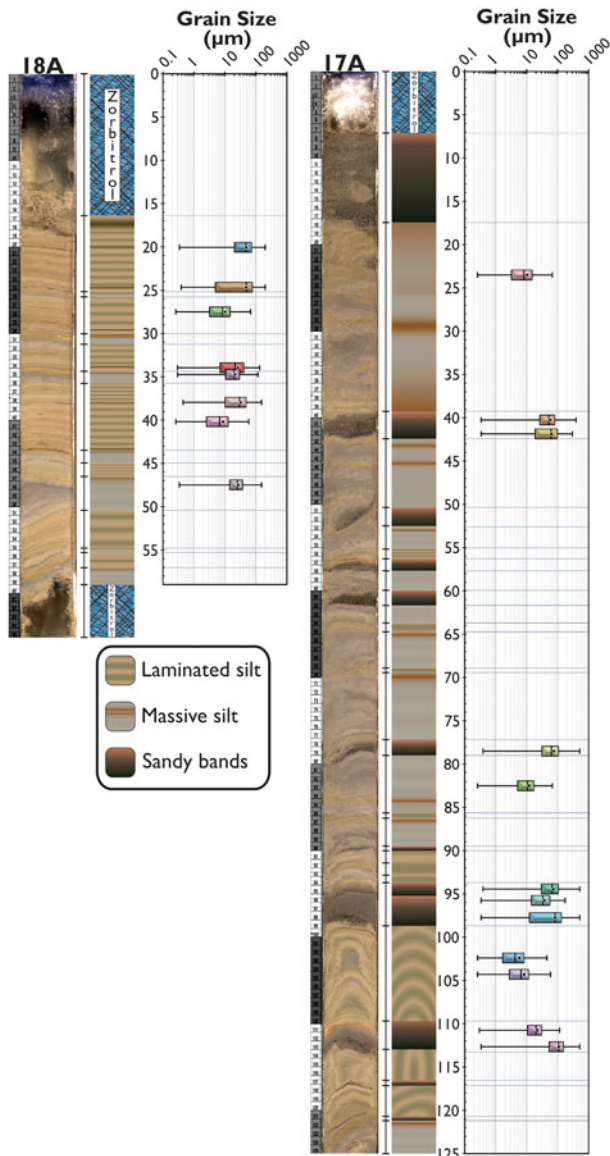


Figure 3. Cores 18A (left) and 17A (right). From left to right: the core image, sediment units, stratigraphic column, and profile of grain-size boxplots. Dashed blue lines delineate units on the profiles. Presented is analysis carried out on silt-to-sand bands, massive silt, and laminated sediments comprehending the main grain-size fractions present in these cores.

Overall, the XRF measurements show both similarities and differences in sediment composition within and between the cores. The sediments from sections 33A-3 and 33A-2 exhibit the highest Ca and lowest K values of the entire analyzed record, including both sandy layers and laminated sediments. On the other hand, the shallower sediments from section 33A-1 and 34A, as well as cores 17A and 18A closer to the Perito Moreno Glacier, display a different compositional trend, with higher K values (Fig. 7).

DISCUSSION

Our detailed analysis of the Canal de los Témpanos cores shows the evolution of the lake system in response to glacier retreat and the influence of Perito Moreno ice-dam outburst events in the sedimentation of Canal de los Témpanos. The sedimentologic,

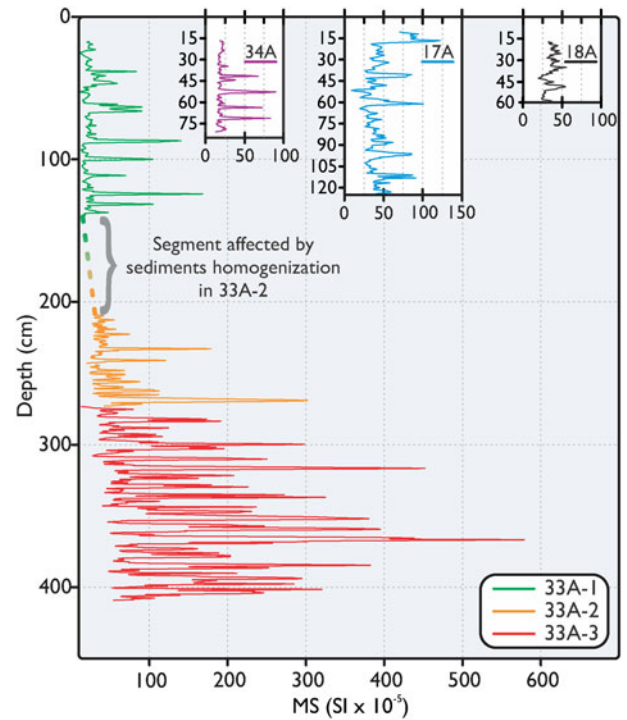


Figure 4. Variation in magnetic susceptibility (MS) with depth in cores 33A, 34A, 17A, and 18A. An increase in MS values towards the deeper sediments is observed through the sections of 33A. This reflects the increase in grain size observed from the top to the bottom of the core.

grain-size, and geochemical data reveal key spatial and temporal changes in the local sedimentary environment.

In particular, we see that: (1) the dominant background sediment grain size in this section of Lago Argentino is fine silt to clay (1–10 µm), interspersed with abundant bands of coarse silt to sand (75–300 µm); (2) there are more than 60 identified coarse silt-to-sand bands consisting of 30 packages with one to eight individual beds each displayed in core 33A, while only 23 outburst flood events were recorded; (3) in core 33A, the abundance of sandy bands decreases towards the top of the core; the thickness, grain-size, and magnetic susceptibility values of these sandy bands also decrease up-core; and (4) XRF analyses reveal two distinct compositional trends, with higher Ca/K in the lower two sections of core 33A and lower Ca/K in the uppermost section of 33A and 17A, 18A, and 34A.

Several key interpretations are therefore immediately evident from these data: (1) there are both more packages of coarse silt-to-sand layers and many more individual coarse silt-to-sand bands than there were Perito Moreno dam-breach floods since the first modern ice-blockage of Canal de los Témpanos was observed in 1917 CE (Guerrido et al., 2014); (2) the abundance of these coarse silt-to-sand bands is greatest in the deepest (oldest) section of the core and decreases towards the surface, suggesting a decreasing source of coarse sediment; and (3) the XRF results show that the uppermost portion of 33A matches the composition of sediment near Perito Moreno (17A and 18A), but that the deeper sections of this core have a different composition. This suggests that the deeper sections of 33A likely have a different dominant sediment source, potentially related to Ameghino Glacier, as we discuss in the following sections.

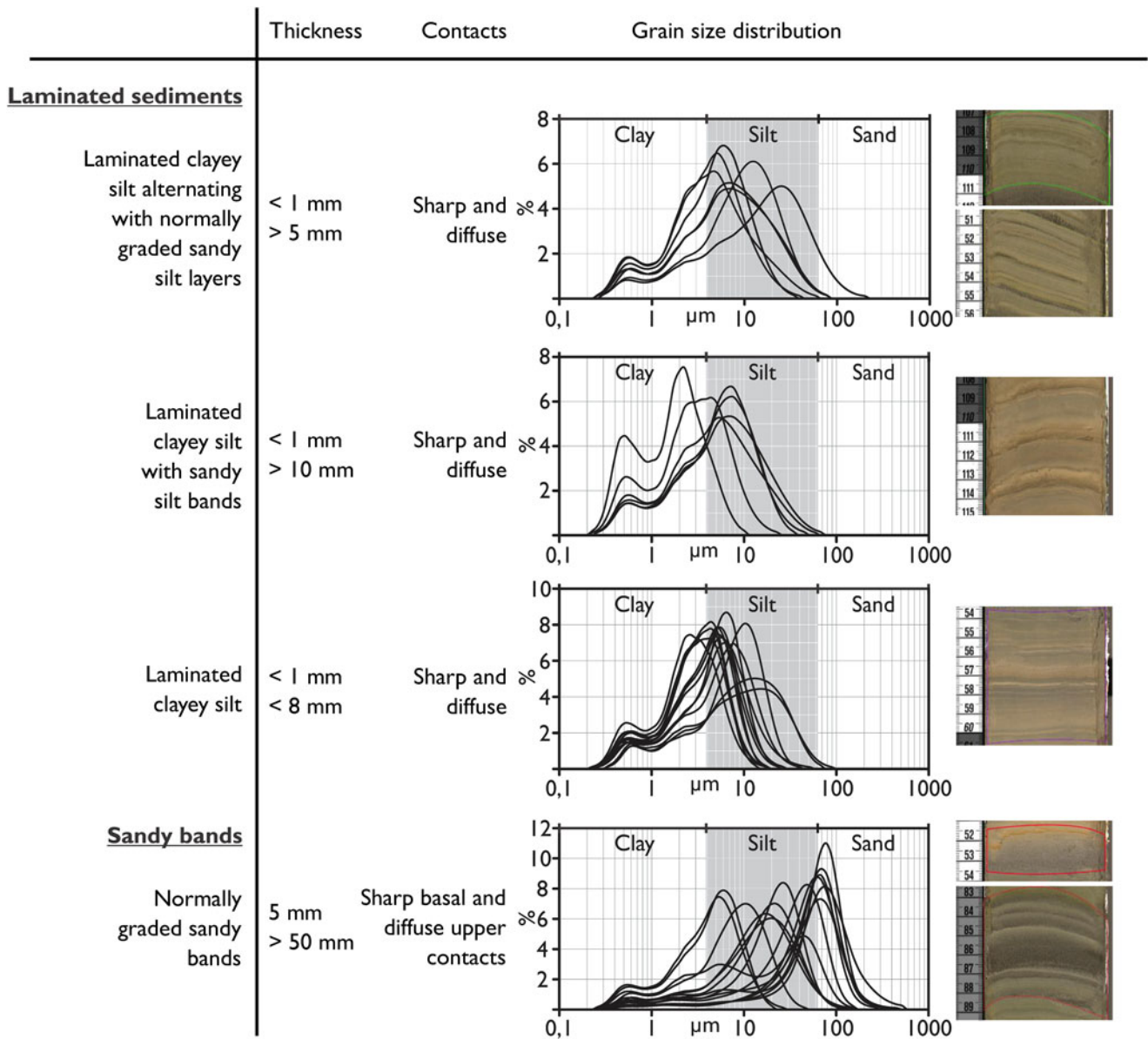


Figure 5. Summary of sedimentary units present in cores 33A and 34A. The coarse fraction (sand) was not fully represented by the grain-size analysis.

Sedimentologic characterization

We observed variations in sediment grain size between laminae, which we attribute to changes in sediment supply reflecting seasonal glacial dynamics. Sediments are transported to the lake from the ablation zone by meltwater flows, categorized as overflows, interflows, or underflows based on their bulk density relative to the lake water (Smith, 1981; Fitzsimons and Howarth, 2018). Coarser sediments (silt with occasional fine sands) at the base of some graded beds likely resulted from rapid deposition by hyperpycnal flows caused by high meltwater discharge during warm seasons (Ashley, 2002; Lamoureux et al., 2002). Finer sediments, such as clayey silt, lacking apparent internal gradation, are transported in suspension by overflows and interflows over longer periods, typically associated with colder seasons (Francus et al., 2008). The absence of coarse grains during cold seasons indicates sedimentation under reduced meltwater input.

Turbidity currents and sandy bands

In cores 33A-2 and 33A-3, we identified repetitive sequences of normally graded sandy bands, interpreted as deposits from subaqueous landslide-triggered turbidity currents. These currents typically move as underflows over extensive distances due to their density contrast with the lake water (Lewis et al., 2002). Landslides can induce additional instabilities in the vicinity, causing successive retrograde landslides until stability is reestablished (Fig. 8A; Mulder and Cochonot, 1996; Mulder and Alexander, 2001). Increased glacial meltwater during summer months can promote hyperpycnal flows capable of carrying coarser and denser sediments, leading to enhanced sedimentation near the source area. High sedimentation rates, rapid deposition, and insufficient consolidation can result in sediment overload. On steep slopes like a delta foreset, a single landslide can trigger one or several turbidity currents that travel significant distances before settling (Bornhold et al., 1994; Mulder and Alexander, 2001).

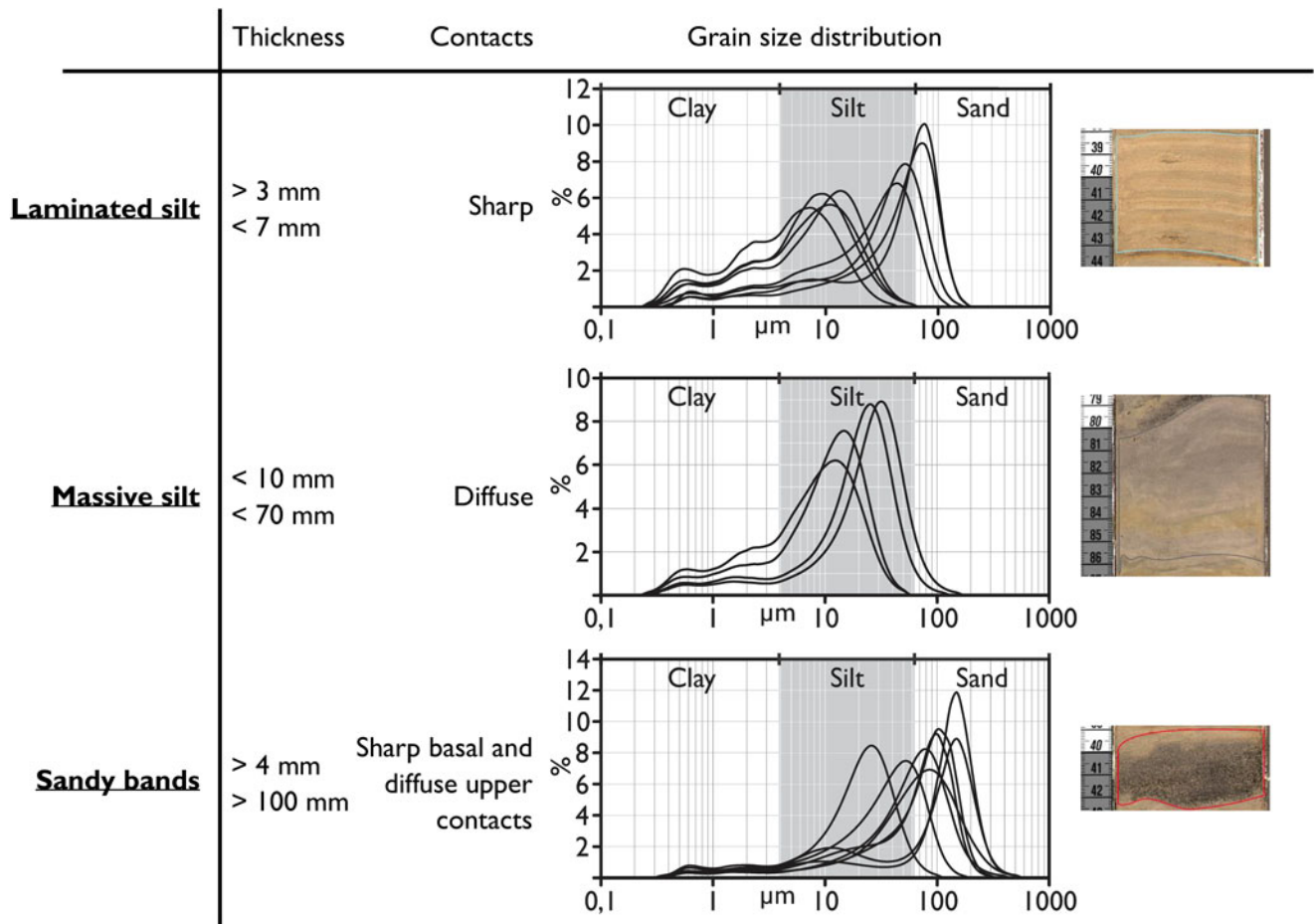


Figure 6. Summary of sedimentary units present in cores 17A and 18A. The coarse fraction (sand) was not fully represented by the grain-size analysis.

In contrast, correlative cores 33A-1 and 34A present isolated sandy bands that are generally thinner, composed of finer grains, and exhibit lower magnetic susceptibility than those in the deeper sections of 33A. Their composition matches that of individual silt-to-sand bands found in cores 17A and 18A near the Perito Moreno glacier front. It is plausible that these bands originate from ice-dam breaches and the associated transport of water and sediments from Brazo Rico to Canal de los Témpanos by the Perito Moreno glacier (Fig. 1), although we cannot securely establish the absolute chronology for each one of these events or compare them to distinctive sediment compositions characteristic of Brazo Rico.

These sedimentologic insights offer valuable perspectives on the dynamic interplay of glacial processes and sedimentation patterns within this complex lake system.

Paleoenvironmental reconstruction

Given the locations of our cores and strong sensitivity of glacial sedimentation to distance from the ice front (Koppes and Hallet, 2002), the observed changes in sediment characteristics are likely influenced by frontal variations of the Perito Moreno and Ameghino glaciers. To better understand these changes, we placed our sedimentary record within the context of glacier fluctuations over recent centuries (Masiokas et al., 2009).

Core 33A-3: proglacial, non-ice-contact environment

In core 33A-3, we observe alternating laminated sediments and sandy bands. Laminated sediments reflect seasonal melt

variations, while sandy bands result from quasi-instantaneous events. These sedimentation patterns are typical of proglacial, non-ice-contact environments where outwash plains terminate in lacustrine deltas, akin to some fjord-type proglacial lakes (Sturm and Matter, 1978; Ashley, 2002; Ballantyne, 2005; Boes et al., 2018).

The two possible sources for the sandy sediments in 33A-3 are Perito Moreno Glacier and Ameghino Glacier. However, a subaqueous moraine associated with the late Herminita glacial advance of Perito Moreno Glacier (Kaplan et al., 2011, 2016; Strelin et al., 2011, 2014; Lodolo et al., 2020) could topographically inhibit the supply of coarse sediments to the 33A site. On the other hand, Ameghino Glacier retreated from its subaerial moraine during the mid-twentieth century (Masiokas et al. 2009), leading to the formation of Laguna Ameghino and isolating its coarse sediment supply from the 33A site. In light of our sedimentary interpretation, the documented glacier retreat (Masiokas et al. 2009), and the down-core compositional divergence across core 33A (upper section 33A-1 is similar to Perito Moreno Glacier cores 17A and 18A while 33A-3 is dissimilar), we could conclude that the sediments in 33A-3 are primarily sourced from Ameghino Glacier and that they should predate the formation of Laguna Ameghino.

Temporal variability in sediment composition

Core 33A-2 has a reduced sand content, a notable decrease in stacked sandy bands, and an increased abundance of laminated

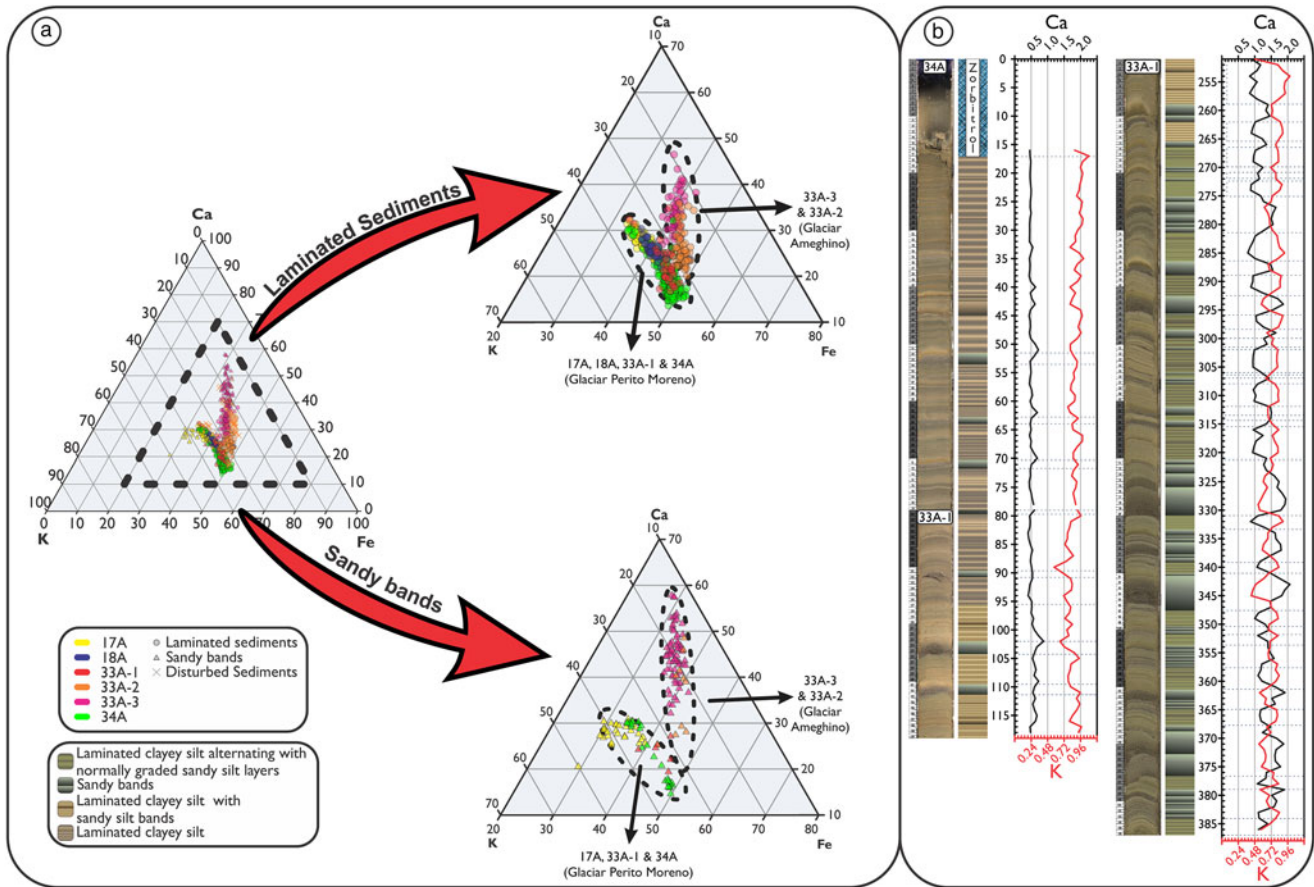


Figure 7. (a) Ternary diagrams illustrating compositional trends. Core sections 33A-2 and 33A-3 reflect a dominant sediment source from Ameghino Glacier, whereas cores 17A, 18A, 33A-1, and 34A predominantly contain sediments from Perito Moreno Glacier. (b) Ca and K profiles relative to core depth and stratigraphy presented for the upper section (composite of cores 34A and 33A-1) and the deeper section (33A-3) of core 33A. These plots illustrate compositional changes along the longer core and between them, highlighting the variations related to the discussed source change.

sediments. Additionally, the upper interval of the cores (section 33A-1 and core 34A) primarily comprises rhythmically laminated pelagic sediments, with fewer individual sandy bands up-core. These changes may be attributed to diminishing water flow energy and decreased sediment supply, suggestive of a more open lacustrine environment, with the glacier source becoming distal, as a result of the retreat of Ameghino Glacier and the development of Laguna Ameghino.

Recent sediments and their sources

Distinct geochemical signatures in sediments can reveal contributions from different inputs. In our core sites, the main sediment sources are Ameghino Glacier and Perito Moreno Glacier; both traverse the Cerro Toro Formation, characterized by shales, sandstones, and turbidites, as well as the El Quemado Complex, consisting of volcanics, acid pyroclastics, sandstones, and claystones. However, Ameghino Glacier uniquely crosses the Bahía de la Lancha Formation, composed of quartzites and low-grade “leptometamorphized” shales (Nulló et al., 2006). Recent sediments found in section 33A-1 and core 34A appear to originate primarily from Perito Moreno Glacier, as their geochemical signature aligns with a similar compositional trend observed in cores 17A and 18A, which exclusively receive sediments from this glacier (Fig. 7). In contrast, older sediments in sections 33A-2 and 33A-3 display a distinct chemical composition, likely reflecting

sediments sourced from Ameghino Glacier prior to the formation of Laguna Ameghino.

These interpreted temporal associations are supported by the only external chronological control made on these cores by Miller et al. (2022) using cesium-137. With this technique, they found the peak of atmospheric radionuclide fallout from 1962 to 1965 CE (García Agudo, 1998) at the bottom of core section 33A-1. This age, marking the onset of the expansion of Laguna Ameghino, is consistent with the sedimentologic and geochemical changes associated with the development of this lake.

Isolated sandy bands and ice-dam rupture events

Isolated sandy bands in 34A and 33A-1 differ in composition from those in sections 33A-2 and 33A-3, although they share a geochemical similarity with cores 17A and 18A. This relation could be consistent with these isolated sandy bands recording Perito Moreno ice-dam rupture events. However, the number of these sandy bands does not match the number of historic ice-dam rupture events, nor does their spacing down-core reflect the known temporal clustering of these events. Therefore, while the geochemical signatures of these bands are potentially consistent with an ice-dam rupture source, we do not find any further evidence for this, and cannot rule out other potential origins. We note that evidence of LIA ice-dam rupture events from Perito

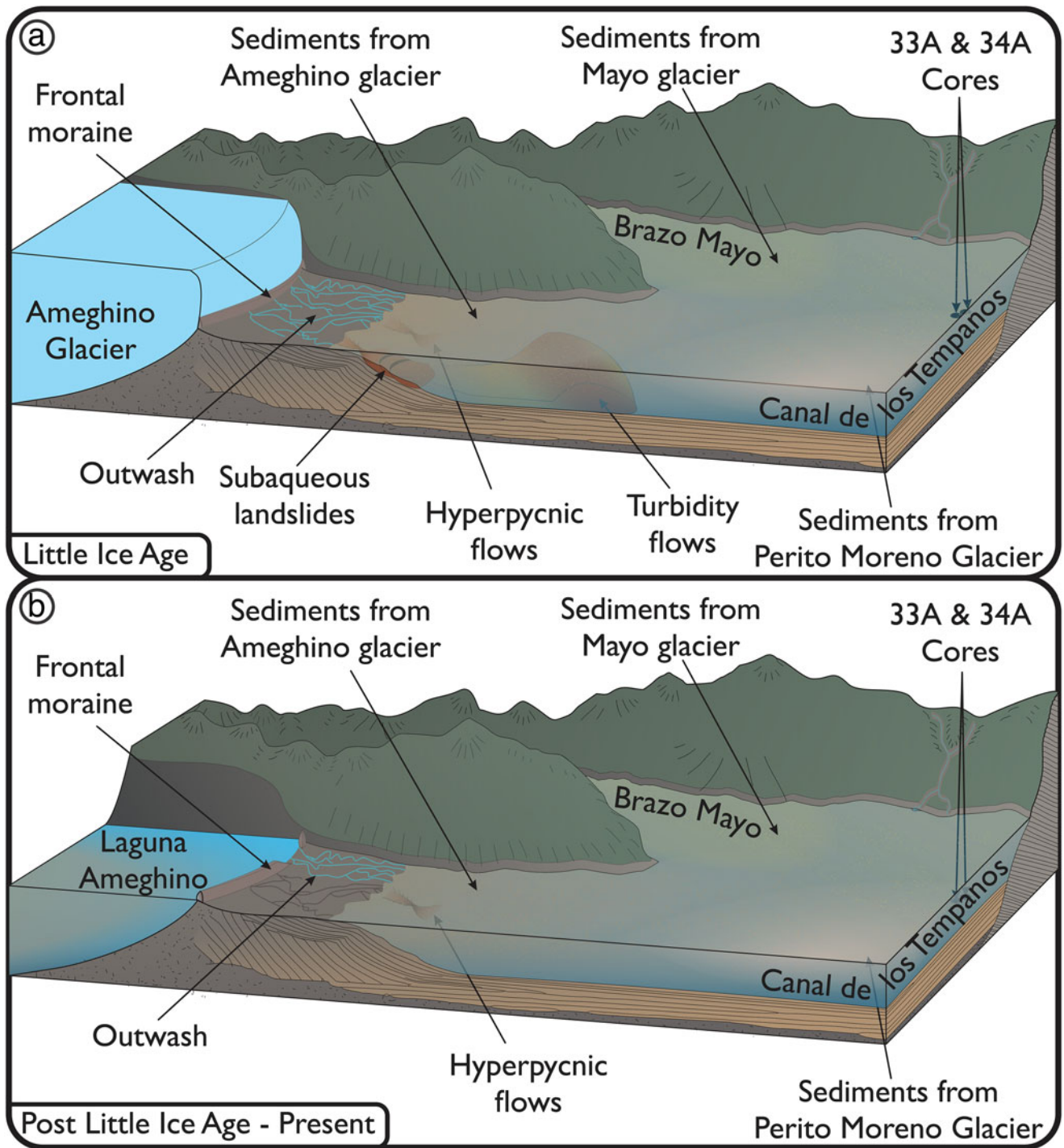


Figure 8. Schematic diagram illustrating the fluvio-glacial plain of Ameghino Glacier and the sedimentary processes occurring in Canal de los Témpanos (adapted from Ballantyne, 2005). (a) shows the situation during the Little Ice Age until the beginning of glacier retreat. (b) shows the situation after the formation of Laguna Ameghino.

Moreno Glacier was detected in the southernmost basin of the Lago Argentino basin, Brazo Sur, which experiences major changes in water level during damming and draining events (Caffau et al., 2021). This suggests that the ice-damming events may primarily affect sedimentation through changes in water level, which are negligible across most of Canal de los Témpanos but significant in some areas of Brazo Rico and Brazo Sur (Pasquini and Depetris, 2011), particularly in small

marginal inlets. Overall, these findings shed light on the sedimentary evidence that may have been produced by different glacier fluctuations.

Broader implications

In this investigation, we delved into the production and deposition of glaciolacustrine sediments within Canal de los

Témpanos, Lago Argentino. We also observed that the remarkable ice-dam rupture occurrences generated by the Perito Moreno glacier, while resulting in the redistribution of substantial volumes of water throughout the lake system, do not leave a pronounced sedimentary imprint and likely have a minor role in the movement of sediment around the lake basin.

These results tie in with and build on our team's work understanding complex glacier lake interactions and their paleoclimatic and paleoenvironmental implications in the Lago Argentino basin (Van Wyk de Vries et al., 2023a, 2023b, 2023c). We showed that the effects of seasonal fluctuations (glacial melt, temperature, and fluvial discharge), that contribute to the formation of varves across the lake basin (Van Wyk de Vries et al., 2021, 2022), are less obvious in the Canal de los Témpanos region of the lake because of numerous silt-to-sand deposits. Our work in the southern branches of Lago Argentino has improved our understanding of the Holocene stratigraphy and glacial moraine record, and provides new constraints on the timing of retreat and sediment redistribution from the main source, Perito Moreno Glacier (e.g. Lodolo et al., 2020; Lozano et al., 2020).

These findings underscore the potential of comprehensive lake core analyses to shed light on regional glacial and sedimentary dynamics, even for intricate systems characterized by multiple competing sources. In our case, the initial working hypothesis—that the energetic Perito Moreno ice-dam outburst events would dominate the sedimentary record in Canal de los Témpanos leaving well-defined turbidity flow deposits—was proven wrong, and the interplay in sedimentation between two glaciers proved to be the dominant signal. Demonstrating this would have been challenging without the length and wide spatial distribution of cores at our disposal. Moreover, our study highlights the utility of sediment records to serve as critical archives for resolving the complex interplay between glacier fluctuations and sedimentation processes, thereby enhancing our understanding of past environmental changes on proglacial landscapes. This knowledge is crucial for interpreting the implications of a warming climate in regions impacted by glacier dynamics.

CONCLUSIONS

Our study provides insight into the sedimentologic, petrophysical, and geochemical changes that have occurred in Canal de los Témpanos over time. We establish temporal associations between these changes and the Late Holocene oscillations of the Perito Moreno and Ameghino glaciers. This work documents the transition in the primary sediment source within our study area, shifting from Ameghino Glacier to Perito Moreno Glacier following the recession of Ameghino Glacier and the formation of the marginal ice-contact lake into which the latter glacier currently calves.

The analysis of cores 33A, 34A, 17A, and 18A has enabled us to develop a conceptual model of the sediment sources in the region, determining that abundant pulses of coarse sediment were deposited in the Canal de los Témpanos during the LIA, when Ameghino Glacier was larger than present. With glacier retreat, once the formation of Laguna Ameghino was initiated, it trapped the glacier's coarse sediment export and limited its input into Lago Argentino. Shortly after, sedimentation in Canal de los Témpanos closely matches the compositional fingerprint of Perito Moreno Glacier sediment output.

Moreover, we do not find a clear signal of the Perito Moreno glacier-dam outburst floods in Lago Argentino, with the largest coarse silt-to-sand bands likely originating from the Ameghino

Glacier delta. Several isolated sand bands in the upper section of core 33A may be produced by these glacier-dam outbursts, but the evidence for this is inconclusive. Overall, our findings contribute to a better understanding of the transient drivers of sedimentary change in this region, and underscore the importance of paleolimnological analyses in reconstructing past environmental changes.

Finally, the recognition of shifts in sediment composition during the LIA and subsequent periods underscores the importance of XRF analysis in detecting changes in sediment sources. This work emphasizes the efficacy of XRF as a tool for identifying such shifts without the requirement for detailed provenance work.

Supplementary material. The supplementary material for this article can be found at <https://doi.org/10.1017/qua.2024.39>

Acknowledgments. We acknowledge the critical role played by the logistical and design expertise of Ryan O'Grady and Anders Noren of the CSD Facility in planning and field phases of this research. Kristina Brady Shannon, Jessica Heck, Alex Stone, and Rob Brown seamlessly coordinated core processing and analytical activities at the CSD Facility. We thank Anastasia Fedotova, Cristina San Martín, Guillermo Tamburini-Beliveau, Alexander Schmies, and Shanti Penprase for their help with core recovery and processing. Pedro Skvarca, scientific director of the Glaciarium Interpretive Center, provided important planning and logistical assistance during initial phases of work. We particularly thank Capitán Alejandro Jaimes for his expert handling of the MV Janet, and for sharing his incisive knowledge of Lago Argentino. We acknowledge Dr. Andrew Wickert for constructive suggestions which improved this manuscript. We also extend our gratitude to Lic. Jorge Strelin for his valuable support and recommendations during the initial stages of this research. This material is based upon work supported by the National Science Foundation under a collaborative research award EAR-1714614 to Wickert, Ito, and Noren, coordinated by Lead PI Maria Beatrice Magnani.

Competing interests. The authors declare that they have no known competing financial interests or personal relationships that could have appeared to influence the work reported in this paper.

REFERENCES

- Abdel Jaber, W., Rott, H., Floricioiu, D., Wuite, J., Miranda, N., 2019. Heterogeneous spatial and temporal pattern of surface elevation change and mass balance of the Patagonian ice fields between 2000 and 2016. *The Cryosphere* **13**, 2511–2535.
- Aniya, M., 1996. Holocene variations of Ameghino Glacier, southern Patagonia. *Holocene* **6**, 247–252.
- Aniya, M., Sato, H., 1995. Morphology of Ameghino Glacier and landforms of Ameghino Valley, southern Patagonia. *Bulletin of Glacier Research* **13**, 69–82.
- Aniya, M., Skvarca, P., 1992. Characteristics and variations of Upsala and Moreno glaciers, southern Patagonia. *Bulletin of Glacier Research* **10**, 39–53.
- Aniya, M., Skvarca, P., 2012. Little ice age advances of Glaciario Perito Moreno, Hielo Patagónico Sur, South America. *Bulletin of Glaciological Research* **30**, 1–8.
- Ashley, G.M., 2002. Glaciolacustrine environments. In: Menzies, J. (Ed.), *Modern and Past Glacial Environments*. Butterworth-Heinemann, Oxford, pp. 335–359.
- Ballantyne, C.K., 2005. Paraglacial landsystems. In: Evans, D.J.A. (Ed.), *Glacial Landsystems*. Routledge, London, pp. 432–460.
- Boes, E., Van Daele, M., Moernaut, J., Schmidt, S., Jensen, B.J.L., Praet, N., Kaufman, D., Haeussler, P., Loso, M.G., De Batist, M., 2018. Varve formation during the past three centuries in three large proglacial lakes in south-central Alaska. *Geological Society of America Bulletin* **130**, 757–774.
- Bornhold, B.D., Ren, P., Prior, D.B., 1994. High-frequency turbidity currents in British Columbia fjords. *Geo-Marine Letters* **14**, 238–243.
- Caffau, M., Lodolo, E., Donda, F., Zecchin, M., Lozano, J.G., Nasi, F., Bran, D.M., Tassone, A., Caburlotto, A., 2021. Stratigraphic signature of the

- Perito Moreno ice-damming during the Little Ice Age (southern Patagonia, Argentina). *Holocene* **32**, 174–182.
- Carrivick, J.L., James, W.H.M., Grimes, M., Sutherland, J.L., Lorrey, A.M., 2020. Ice thickness and volume changes across the Southern Alps, New Zealand, from the little ice age to present. *Scientific Reports* **10**, 13392. <https://doi.org/10.1038/s41598-020-70276-8>
- Carrivick, J.L., Tweed, F.S., 2013. Proglacial lakes: character, behaviour and geological importance. *Quaternary Science Reviews* **78**, 34–52.
- Cohen, A.S., 2003. *Paleolimnology: The History and Evolution of Lake Systems*. Oxford University Press, New York.
- Davies, B.J., Glasser, N.F., 2012. Accelerating shrinkage of Patagonian glaciers from the Little Ice Age (~AD 1870) to 2011. *Journal of Glaciology* **58**, 1063–1084.
- De Angelis, H., 2014. Hypsometry and sensitivity of the mass balance to changes in equilibrium-line altitude: the case of the Southern Patagonia Icefield. *Journal of Glaciology* **60**, 14–28.
- Fedotova, A., Magnani, M.B., 2021. Seismic stratigraphy of neoglacial ice fluctuations in Lago Argentino (Patagonia, Argentina). *AGU Fall Meeting 2021, New Orleans, Louisiana, December 13–17, 2021*, EP15A-08. <https://ui.adsabs.harvard.edu/abs/2021AGUFM15A..08F/abstract>
- Fitzsimons, S., Howarth, J., 2018. Glaciolacustrine processes. In: Menzies, J., van der Meer, J.J.M. (Eds.), *Past Glacial Environments (Second Edition)*. Elsevier, Amsterdam, pp. 309–334.
- Francus, P., Bradley, R.S., Lewis, T., Abbott, M., Retelle, M., Stoner, J.S., 2008. Limnological and sedimentary processes at Sawtooth Lake, Canadian High Arctic, and their influence on varve formation. *Journal of Paleolimnology* **40**, 963–985.
- García Agudo, E., 1998. Global distribution of ^{137}Cs inputs for soil erosion and sedimentation studies. In: International Atomic Energy Agency (Ed.), *Use of ^{137}Cs in the Study of Soil Erosion and Sedimentation*. IAEA-TECDOC-1028. International Atomic Energy Agency, Vienna, pp. 117–121.
- Garreaud, R.D., Vuille, M., Compagnucci, R., Marengo, J., 2009. Present-day South American climate. *Palaeogeography, Palaeoclimatology, Palaeoecology* **281**, 180–195.
- Garreaud, R., Lopez, P., Minvielle, M., Rojas, M., 2013. Large-scale control on the Patagonian climate. *Journal of Climate* **26**, 215–230.
- Goyenechea, C., 2017. *EIA Aprovechamientos Hidroeléctricos del Río Santa Cruz (Presidente Dr. Néstor C. Kirchner y Gobernador Jorge Cepernic, Provincia de Santa Cruz*. Serman & Asociados S.A., Buenos Aires.
- Guerrido, C.M., Villalba, R., Rojas, F., 2014. Documentary and tree-ring evidence for a long-term interval without ice impoundments from Glaciar Perito Moreno, Patagonia, Argentina. *Holocene* **24**, 1686–1693.
- Harrison, S., Kargel, J.S., Huggel, C., Reynolds, J., Shugar, D.H., Betts, R.A., Emmer, A., et al., 2018. Climate change and the global pattern of moraine-dammed glacial lake outburst floods. *Cryosphere* **12**, 1195–1209.
- Kaplan, M.R., Schaefer, J.M., Strelin, J.A., Denton, G.H., Anderson, R.F., Vandergoes, M.J., Finkel, R.C., et al., 2016. Patagonian and southern South Atlantic view of Holocene climate. *Quaternary Science Reviews* **141**, 112–125.
- Kaplan, M.R., Strelin, J.A., Schaefer, J.M., Denton, G.H., Finkel, R.C., Schwartz, R., Putnam, A.E., Vandergoes, M.J., Goehring, B.M., Travis, S.G., 2011. In-situ cosmogenic ^{10}Be production rate at Lago Argentino, Patagonia: implications for late-glacial climate chronology. *Earth and Planetary Science Letters* **309**, 21–32.
- Koppes, M.N., Hallet, B., 2002. Influence of rapid glacial retreat on the rate of erosion by tidewater glaciers. *Geology* **30**, 47–50.
- Lamoureux, S.F., Gilbert, R., Lewis, T., 2002. Lacustrine sedimentary environments in High Arctic proglacial Bear Lake, Devon Island, Nunavut, Canada. *Arctic, Antarctic, and Alpine Research* **34**, 130–141.
- Lenaerts, J.T.M., Van Den Broeke, M.R., Van Wessem, J.M., Van De Berg, W.J., Van Meijgaard, E., Van Ulft, L.H., Schaefer, M., 2014. Extreme precipitation and climate gradients in Patagonia revealed by high-resolution regional atmospheric climate modeling. *Journal of Climate* **27**, 4607–4621.
- Lewis, T., Gilbert, R., Lamoureux, S.F., 2002. Spatial and temporal changes in sedimentary processes at Proglacial Bear Lake, Devon Island, Nunavut, Canada. *Arctic, Antarctic, and Alpine Research* **34**, 119–129.
- Lodolo, E., Donda, F., Lozano, J., Baradello, L., Romeo, R., Bran, D.M., Tassone, A., 2020. The submerged footprint of Perito Moreno glacier. *Scientific Reports* **10**, 16437. <https://doi.org/10.1038/s41598-020-73410-8>
- Lozano, J., Donda, F., Bran, D., Lodolo, E., Baradello, L., Romeo, R., Vilas, J.F., Grossi, M., Tassone, A., 2020. Depositional setting of the southern arms of Lago Argentino (southern Patagonia). *Journal of Maps* **16**, 324–334.
- Magnani, M.B., Fedotova, A., Peterson, D.E., MacPhail, M.D., 2019. Constraints on glacial isostatic adjustment in the Southern Patagonia Icefield from high-resolution seismic reflection imaging of glacial lacustrine deposits in the Lago Argentino, Argentina. *AGU Fall Meeting 2019, San Francisco, California, December 9–13, 2019*, C21F-1516. <https://ui.adsabs.harvard.edu/abs/2019AGUFM.C21F1516M/abstract>
- Masiokas, M.H., Rivera, A., Espizua, L.E., Villalba, R., Delgado, S., Aravena, J.C., 2009. Glacier fluctuations in extratropical South America during the past 1000 years. *Palaeogeography, Palaeoclimatology, Palaeoecology* **281**, 242–268.
- Mercer, J.H., 1968. Variations of some Patagonian glaciers since the Late-Glacial. *American Journal of Science* **266**, 91–109.
- Miller, L., MacGregor, K., Van Wyk de Vries, M., Ito, E., Shapley, M.D., Brignone, G., Romero, M., 2022. Using cesium-137 to determine sedimentation patterns in two proglacial lakes – Lago Argentino, Southern Patagonian icefield, Argentina, and Lake Josephine, Glacier National Park, Montana, USA. *Geological Society of America Abstracts with Programs* **54**(5). <https://doi.org/10.1130/abs/2022AM-377913>
- Minowa, M., Sugiyama, S., Sakakibara, D., Sawagaki, T., 2015. Contrasting glacier variations of Glaciar Perito Moreno and Glaciar Ameghino, Southern Patagonia Icefield. *Annals of Glaciology* **56**, 26–32.
- Mulder, T., Alexander, J., 2001. The physical character of subaqueous sedimentary density flow and their deposits. *Sedimentology* **48**, 269–299.
- Mulder, T., Cochonat, P., 1996. Classification of offshore mass movements. *Journal of Sedimentary Research* **66**, 43–57.
- Nullo, F., Blasco, C., Rizzo, C., Combina, A., Otamendi, J., 2006. *Hoja Geológica 5172-I y 5175-II El Calafate, Provincia de Santa Cruz*. Instituto de Geología y Recursos Minerales, Servicio Geológico Minero Argentino, Bulletin 396, Buenos Aires.
- Pasquini, A.I., Depetris, P.J., 2011. Southern Patagonia's Perito Moreno Glacier, Lake Argentino, and Santa Cruz River hydrological system: an overview. *Journal of Hydrology* **405**, 48–56.
- Piret, L., Bertrand, S., Nguyen, N., Hawkings, J., Rodrigo, C., Wadham, J., 2022. Long-lasting impacts of a 20th century glacial lake outburst flood on a Patagonian fjord-river system (Pascua River). *Geomorphology* **399**, 108080. <https://doi.org/10.1016/j.geomorph.2021.108080>
- Rabassa, J., Coronato, A.M., Salemme, M., 2005. Chronology of the Late Cenozoic Patagonian glaciations and their correlation with biostratigraphic units of the Pampean region (Argentina). *Journal of South American Earth Sciences* **20**, 81–103.
- Reed, J.A., 2007. *The Paleontological Stratigraphic Interval Construction and Analysis Tool*. Master's thesis, Iowa State University, Ames, Iowa. <https://doi.org/10.31274/rtd-180813-16237>
- Richter, A., Mardewald, E., Hormacocha, J.L., Mendoza, L., Perdomo, R., Connon, G., Scheinert, M., Horwath, M., Dietrich, R., 2016. Lake-level variations and tides in Lago Argentino, Patagonia: insights from pressure tide gauge records. *Journal of Limnology*, **75**, 62–77.
- Rott, H., Stuefer, M., Nagler, T., Riedl, P.C., 2004. Recent fluctuations and damming of glacial Perito Moreno, Patagonia, observed by means of ERS and Envisat imagery. In: Lacoste, H., Ouwehand, L. (Eds.), *Proceedings of the 2004 Envisat & ERS Symposium, Salzburg, Austria, September 6–10, 2004*. European Space Agency, Noordwijk.
- Schnurrenberger, D., Russell, J., Kelts, K., 2003. Classification of lacustrine sediments based on sedimentary components. *Journal of Paleolimnology* **29**, 141–154.
- Shugar, D.H., Burr, A., Haritashya, U.K., Kargel, J.S., Watson, C.S., Kennedy, M.C., Bevington, A.R., Betts, R.A., Harrison, S., Strattman, K., 2020. Rapid worldwide growth of glacial lakes since 1990. *Nature Climate Change* **10**, 939–945.
- Smith, N.D., 1981. The effect of changing sediment supply on sedimentation in a glacier-fed lake. *Arctic & Alpine Research* **13**, 75–82.
- Smol, J.P., 1992. Paleolimnology: an important tool for effective ecosystem management. *Journal of Aquatic Ecosystem Health* **1**, 49–58.

- Strelin, J.A., Denton, G.H., Vandergoes, M.J., Ninnemann, U.S., Putnam, A.E.**, 2011. Radiocarbon chronology of the late-glacial Puerto Bandera moraines, Southern Patagonian Icefield, Argentina. *Quaternary Science Reviews* **30**, 2551–2569.
- Strelin, J.A., Kaplan, M.R., Vandergoes, M.J., Denton, G.H., Schaefer, J.M.**, 2014. Holocene glacier history of the Lago Argentino basin, Southern Patagonian Icefield. *Quaternary Science Reviews* **101**, 124–145.
- Strelin, J.A., Malagnino, E.C.**, 1996. Glaciaciones Pleistocenas del Lago Argentino y Alto Valle del Río Santa Cruz. *XIII Congreso Geológico Argentino y III Congreso de Exploración de Hidrocarburos, Actas IV* (January 1996). XIII Congreso Geológico Argentino, Buenos Aires, Argentina, pp. 311–325.
- Sturm, M., Matter, A.**, 1978. Turbidites and varves in Lake Brienz (Switzerland): deposition of clastic detritus by density currents. In: Matter, A., Tucker, M.E. (Eds.), *Modern and Ancient Lake Sediments*. International Association of Sedimentologists Special Publication 2. Blackwell Scientific Publications, Oxford, pp. 147–168.
- Sugiyama, S., Minowa, M., Sakakibara, D., Skvarca, P., Sawagaki, T., Ohashi, Y., Naito, N., Chikita, K.**, 2016. Thermal structure of proglacial lakes in Patagonia. *Journal of Geophysical Research: Earth Surface* **121**, 2270–2286.
- Sugiyama, S., Skvarca, P., Naito, N., Enomoto, H., Tsutaki, S., Tone, K., Marinsek, S., Aniya, M.**, 2011. Ice speed of a calving glacier modulated by small fluctuations in basal water pressure. *Nature Geoscience* **4**, 597–600.
- Sutherland, J.L., Carrivick, J.L., Gandy, N., Shulmeister, J., Quincey, D.J., Cornford, S.L.**, 2020. Proglacial lakes control glacier geometry and behavior during recession. *Geophysical Research Letters* **47**, e2020GL088865. <https://doi.org/10.1029/2020GL088865>
- Tweed, F.S., Carrivick, J.L.**, 2015. Deglaciation and proglacial lakes. *Geology Today* **31**, 96–102.
- Van Wyk de Vries, M., Ito, E., Romero, M., Shapley, M., Brignone, G.**, 2023a. Periodicity of the Southern Annular Mode in Southern Patagonia, insight from the Lago Argentino varve record. *Quaternary Science Reviews* **304**, 108009, <https://doi.org/10.1016/j.quascirev.2023.108009>
- Van Wyk de Vries, M., Ito, E., Shapley, M., Brignone, G.**, 2021. Semi-automated counting of complex varves through image autocorrelation. *Quaternary Research* **104**, 89–100.
- Van Wyk de Vries, M., Ito, E., Shapley, M., Brignone, G., Romero, M., Wickert, A.D., Miller, L.H., MacGregor, K.R.**, 2022. Physical limnology and sediment dynamics of Lago Argentino, the world's largest ice-contact lake. *Journal of Geophysical Research: Earth Surface* **127**, e2022JF006598. <https://doi.org/10.1029/2022JF006598>
- Van Wyk de Vries, M., Ito, E., Shapley, M., Romero, M., Brignone, G.**, 2023b. Investigating paleoclimate and current climatic controls at Lago Argentino using sediment pixel intensity time series. *Journal of Paleolimnology* **70**, 311–330.
- Van Wyk De Vries, M., Romero, M., Penprase, S.B., Ng, G.-H.C., Wickert, A.D.**, 2023c. Increasing rate of 21st century volume loss of the Patagonian Icefields measured from proglacial river discharge. *Journal of Glaciology* **69**, 1187–1202.
- Veh, G., Korup, O., Walz, A.**, 2020. Hazard from Himalayan glacier lake outburst floods. *Proceedings of the National Academy of Sciences of the United States of America* **117**, 907–912.
- Warren, C.R.**, 1994. Freshwater calving and anomalous glacier oscillations: recent behaviour of Moreno and Ameghino Glaciers, Patagonia. *Holocene* **4**, 422–429.